INTERNATIONAL JOURNAL OF RESEARCH
In Advanced Engineering Technologies

Volume 3, Issue 5 DEC 2014

SENSORLESS INDUCTION MOTOR DRIVES WITH WIDE-SPEED-RANGE ESTIMATION

P. SRINIVASA PAVAN KUMAR
B.tech q/s institute of technology, vengamukkala palem, ongole, dist prakasam A.P, India,
Mail Id: srinivaspavan242@gmail.com

T. CHANDRA BABU
M.tech (assistant proffesor), q/s institute of technology, vengamukkala palem, ongole
prakasam A.P, India
Mail Id:Chandra.qisit@gmail.com

ABSTRACT—Parallel identification schemes for both speed and stator resistance of sensor less induction motor drives are proposed for a wide range of speed estimation. Recently, the development of speed estimation methods for sensor less control of induction motor drives has found great interest in the research community. Parameter adaptation schemes play an important role for better speed estimation over a wide range from zero to high levels beyond the rated speed These estimation algorithms combine a sliding-mode current observer with Popov's hyper stability theory. Low- and zero-speed operations of the proposed sliding mode-observer (SMO)-based speed estimation combined with an online stator resistance adaptation scheme are investigated. A modified SMO-based speed estimation scheme for field-weakening operation is also introduced. The mismatch problem of magnetizing inductance in the field-weakening region is treated by an online identification scheme. Magnetizing inductance, estimated in this way, is further utilized within the SMO, so that the main flux saturation variation is taken into consideration. The performance of the proposed SMO and its speed estimation accuracy, with an indirect field-oriented controlled induction motor, are verified by simulation and experimental results over a wide speed range from zero to high values beyond the base speed.

Index Terms—Magnetizing inductance identification, slidingmode observer (SMO), speed sensorless, stator resistance identification

1.INTRODUCTION

Several methods have been recently proposed for speed estimation of sensor less induction motor drives .They can be classified into two major categories. The first one includes the techniques that estimate the rotor speed based onnon ideal phenomena such as rotor slot harmonics and high frequency signal injection methods. Such methods require spectrum analysis which, besides being time-consuming procedures, allows a narrow band of speed control. The second category of speed estimation methods relies on the model of the induction motor. The supremacy of a certain method depends on its estimation accuracy over a wide speed range. Model based methods of speed estimation are characterized by their simplicity, but sensitivity to parameter variations is considered the major problem associated with them. Stator resistance plays an important role, and its value has to be known with good precision in order to obtain accurate speed estimation in the low-speed region.

The interest in stator resistance adaptation came on the scene much recently; with the advances of speed sensor less systems. It has also received more attention with the introduction of the direct torque control technique. An accurate value of the stator resistance is of crucial importance for the correct operation of a sensor less drive in the low-speed region, since any mismatch between the actual value and the set value used within the model of speed estimation may lead not only to a substantial speed estimation error but also to instability. Therefore, there is a great interest in the research community to develop stator resistance identification schemes for accurate low-speed estimation. An offline estimation procedure of the motor parameters at various operating conditions is introduced.

In that work, the stator resistance is observed to be varying as a function of stator temperature. The rotor resistance is also estimated offline for rotor field orientation as a function of slip frequency and rotor temperature. Numerous online estimation techniques are also proposed for continuously updating parameter values. Online rotor resistance estimation for rotor field orientation using a sliding mode observer (SMO) and a model reference adaptive system (MRAS) is proposed in. The online stator resistance identification schemes can be classified into a couple of distinct categories. These schemes rely on stator current measurement and mostly require information regarding stator voltages. The first category includes different types of estimators which often use an adaptive mechanism to update the value of stator resistance. The stator resistance is determined in by using a reactive-power-based MRAS.

The reactive power relies on the accuracy of other parameters, such as leakage inductance and rotor resistance, which are not necessarily constant, and the result is prone to error. Adaptive full-order flux observers (AFFOs) for estimating the speed and stator resistance are developed using Lyapunov's stability criterion. While these schemes are not computationally intensive, an AFFO with a nonzero gain matrix may become unstable. An MRAS for estimating the speed and stator resistance is developed using Popov's stability criterion. Recently, two extended Kaman filter (EKF) algorithms for estimating stator and rotor resistances are utilized in a braided manner, thus achieving an accurate estimation of a high number of parameters and states than would have been possible with single EKF algorithm. The second category of online stator resistance identification schemes depends on artificial intelligence techniques in the process of stator resistance adaptation. Artificial neural networks for estimating stator and rotor resistances are used for this purpose

High-performance applications of sensor less systems require high accuracy of speed estimation over a wide speed range extending from very low and zero-speed operations to high speeds beyond the rating. Operation of field-oriented induction motors below the base speed is usually achieved with constant flux. Therefore, magnetizing inductance can be regarded as constant and equal to its rated value. In the field-weakening region, the rotor flux reference has to be reduced below its rated value. Variation of the rotor flux reference implies variable level of saturation, and consequently, magnetizing inductance of the machine is varied. Accurate value of magnetizing inductance is of utmost importance for many reasons.

The first one is the correct setting of the d-axis stator currenteference in a vector-controlled drive. The second one is its importance for accurate speed estimation in the field-weakening region, using machine-model-based approaches, of sensor less systems. The third reason is the dependency of rotor time v constant identification schemes on magnetizing inductance, such as the method utilizing reactive power. The accurate estimation of rotor time constant in the field-weakening region requires a correct value of the magnetizing inductance tube known.

This method is characterized by its simplicity and accuracy; therefore, it issued here with the proposed SMO to improve speed estimation in the field-weakening region. This paper presents a speed estimation algorithm based on a sliding-mode current observer which combines variable structure control, is used for implementing the proposed smashed estimation algorithm. Experimental results are presented along with those obtained by simulation to evaluate the accuracy of the proposed SMO over a wide speed range from zero to high values beyond the base speed.

2. SPEED AND STATOR RESISTANCE ESTIMATION PROCEDURE

The induction motor can be represented by its dynamic model expressed in the stationary reference frame in terms of stator current and rotor flux as follows

$$\frac{d}{dt}\begin{bmatrix} i_s^s \\ \lambda_r^s \end{bmatrix} = \begin{bmatrix} A_{11} & A_{12} \\ A_{21} & A_{22} \end{bmatrix}\begin{bmatrix} i_s^s \\ \lambda_r^s \end{bmatrix} + \begin{bmatrix} b_1 \\ 0 \end{bmatrix}[v_s^s] = A_x + Bv_s \quad (1)$$

WhereA11 , A12, A21A22, and b1are given in the Appendix. With reference to the introduced mathematical model and considering the stator currents as the system outputs, the sliding-mode current observer can be constructed as

$$pi\hat{}_s^s = A\hat{}_{11} i\hat{}_s^s + A\hat{}_{12}\lambda\hat{}_r^s + b_1 v_s^s + Ksgn(i\hat{}_s^s - i_s^s) \quad (2)$$

$$p\lambda\hat{}_r^s = A_{21} i\hat{}_s^s + A\hat{}_{22}\lambda\hat{}_r^s \quad (3)$$

Where K is the switching gain. The error equation which takes into account parameter variation can be expressed, by subtracting (1) from (2), as follows

$$\frac{de_i}{dt} = A_{11} e_i + A_{12} e_\lambda + \Delta A_{11} i\hat{}_s^s + \Delta A_{12}\lambda\hat{}_r^s + Ksgn(i\hat{}_s^s - i_s^s) \quad (4)$$

Where

$$e_i = i\hat{}_s^s - i_s^s, e_\lambda = \lambda\hat{}_r^s - \lambda_r^s, \Delta A = \begin{bmatrix} \Delta A_{11} & \Delta A_{12} \\ \Delta A_{21} & \Delta A_{22} \end{bmatrix}.$$

The sliding surface S is constructed

$$S(t) = e_i = i\hat{}_s^s - i_s^s = 0 \quad (5)$$

Where as the switching function of SMO is defined as

$$\text{sgn}(s) = \begin{cases} 1 & \text{if } S \geq 0 \\ -1 & \text{if } S < 0 \end{cases}. \quad (6)$$

If rotor speed and stator resistance are considered as variable parameters, assuming no other parameter variations, the matrix ΔA is expressed as follows

$$\Delta A_{11} = \frac{-\Delta R_s I}{\sigma L_s}$$

$$\Delta A_{12} = \frac{-\Delta\omega_r J}{\mathcal{E}}$$

$$\Delta A_{21} = 0$$

$$\Delta A_{22} = \Delta\omega_r J.$$

The sliding mode occurs when the following sliding condition is satisfied

$$e_i^T . e_i < 0. \qquad (7)$$

A.CHARACTERISTICS OF SMO ON SLIDING SURFACE

When the estimation error trajectory reaches the sliding surface, i.e. =0, then, from, it is obvious that the observed currents will converge to the actual ones, i.e $i\hat{}_s^s = i_s^s$. According to the equivalent control concept, assuming that the observed currents ˆis match the actual currents sin thsteady state, then

$$e_i^T = e_i = 0 \qquad (8)$$

From which the error equation becomes

$$0 = A_{12} e_\lambda + \Delta A_{11} i\hat{}_s^s + \Delta A_{12} \lambda\hat{}_r^s - L. \qquad (9)$$

The estimation algorithm of stator currents is constructed by a closed-loop observer, as in, whereas the estimation of rotor fluxes is carried out by an open loop represented by without the flux error. Therefore, the real and estimated rotor fluxes are assumed the same ˆ $\lambda\hat{}_r^s = \lambda_r^s$; thus, the error equation becomes as follows:

$$0 = \Delta A_{11} i\hat{}_s^s + \Delta A_{12} \lambda\hat{}_r^s - L. \qquad (10)$$

B.STABILITY OF THE IDENTIFICATION SYSTEM

Popov's hyper stability theory is well known as stability criterion for nonlinear feedback systems. This theory is applied hereto examine the stability of the proposed identification system. This requires that the error system and the feedback system are derived so that the theory could be applied. In the SMO, using a speed identification error$\Delta\omega_r = \omega\hat{}_r - \omega_r$, a stator resistance identification error$\Delta R_s = R\hat{}_s - R_s$, and an error signal $L = -Ksgn(i\hat{}_s^s - i_s^s)$ the error system written as

$$L = \Delta A_{11} i\hat{}_s^s + \Delta A_{12} \lambda\hat{}_r^s \qquad (11)$$

Substituting the given equivalents of ΔA_{11} andΔA_{12} into (11) yields

$$L = -\frac{\Delta R_s}{\sigma L_s} i\hat{}_s^s - \frac{\Delta\omega_r J}{\mathcal{E}} \lambda\hat{}_r^s = -z_1 \Delta R_s - z_2 \Delta\omega_r \qquad (12)$$

Where

$$z_1 = (1/\sigma L_s) i\hat{}_s^s \qquad (13)$$

$$z_2 = (J/\mathcal{E}) \lambda\hat{}_r^s \qquad (14)$$

Popove's integral inequality of (11) is written as follows [14]

$$S = \int_0^{t_0} L^T W dt \geq -\gamma^2, \quad \gamma = const \qquad (15)$$

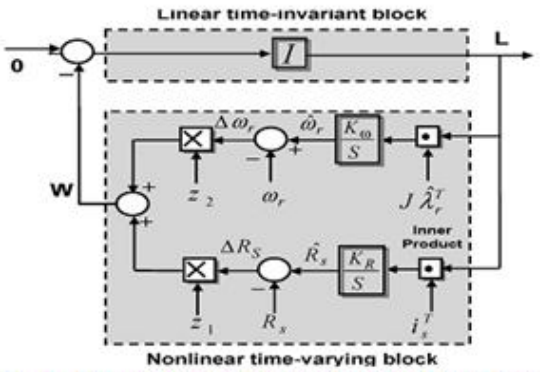

Fig. 1. Identification system for speed and stator resistance.

Where L^T is the input vector;$W = -z_1 \Delta R_s - z_2 \Delta R_s - z_2 \omega_r$, which represents the nonlinear block, is the output vector of the feedback block; and γ is a finite positive constant which does not depend ont0

$$S = \int_0^{t_0} L^T (-z_1 \Delta R_s - z_2 \Delta\omega_r) dt \qquad (16)$$

Substituting (13) and (14) into (16) yields

$$S = \int_0^{t_0} L^T W dt$$

$$= \int_0^{t_0} \left(\frac{-L^T \Delta R_s}{\sigma L_s} i\hat{}_s^s\right) dt + \left(\frac{-L^T \Delta\omega_s J}{\omega} \lambda\hat{}_s^s\right) dt \qquad (17)$$

$$S = S_1 + S_2 \geq -\gamma^2 \qquad (18)$$

$$S_1 = \int_0^{t_0} \left(\frac{-L^T \Delta R_s}{\sigma L_s} i\hat{}_s^s\right) dt \geq -\gamma_1^2 \qquad (19)$$

$$S_2 = \int_0^{t_0} \left(\frac{-L^T \Delta\omega_s J}{\omega} \lambda\hat{}_s^s\right) dt \geq -\gamma_2^2 \qquad (20)$$

The validity of Popov's inequality of (18) can be verified by means of the inequalities expressed by (19) and (20), provided that the estimates of rotor speed and stator resistance can be obtained by and, respectively,

$$\omega\hat{}_r = K_\omega \int L^T J \lambda\hat{}_r dt \qquad (21)$$

$$R\hat{}_s = K_R \int L^T i_s^s dt \qquad (22)$$

Where K_ω and K_R are adaptive gains.

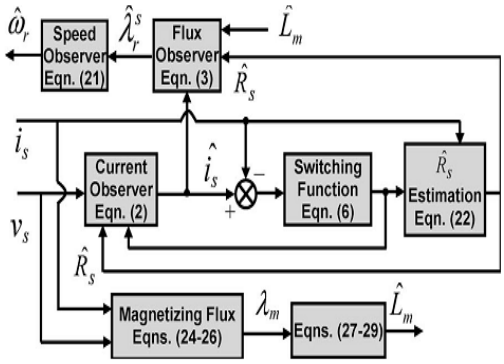

Fig. 2. Block diagram of speed, stator resistance, and magnetizing inductance identification schemes

An identification system for speed and stator resistance is shown in Fig. 1, which is constructed from a linear time-invariant forward block and a nonlinear time-varying feedback block. The system is hyper stable if the forward block I positive real and the input and output of the nonlinear feedback block satisfy Popov's integral inequality. Fig. 2 shows the block diagram of parallel speed and stator resistance estimation algorithms based on a combination of SMO and Popov's hyper stability theory.

3 ON LINE IDENTIFICATION ALGORITHM OF MAGNETIZING INDUCTANCE

Magnetizing inductance of induction motors may vary significantly when the rotor flux reference varies in the field weakening region. Accurate speed estimation in this region requires the precise value of magnetizing inductance. Therefore, the structure of the speed observer should be modified in such a way that the variation of main flux saturation is recognized within the speed estimation algorithm. This requires the online identification algorithm of the magnetizing inductance. The magnetizing inductance is given on the basis of the known magnetizing curve of the machine with

$$\bar{L}_m = \lambda_m / i_m \qquad (23)$$

Where

$$\lambda_m = \sqrt{\lambda_{dm}^2 + \lambda_{qm}^2} \qquad (24)$$

The magnetizing flux vector can be obtained as follows

$$\lambda_{dm} = \int (v_{ds} - R_s i_{ds})dt - L_s i_{ds}. \qquad (25)$$

$$\lambda_{qm} = \int (v_{qs} - R_s i_{qs})dt - L_s i_{qs}. \qquad (26)$$

Since the magnetizing flux is now known, it is possible to estimate the magnetizing inductance using the known nonlinear inverse magnetizing curve

$$i_m = f(\lambda_m) \qquad (27)$$

$$\hat{L}_m = \frac{\lambda_m}{i_m} \qquad (28)$$

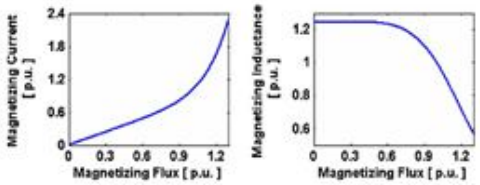

Fig. 3. Magnetizing curve and magnetizing inductance variation of the machine used in experiments

The block diagram of online identification procedures of the magnetizing inductance is shown in Fig. 2. The magnetizing curve of the machine was identified offline, as described in, and is represented with a suitable analytical function in per unit, of the form

$$i_{m(pu)} = a\lambda_{m(pu)} + (1-a)\lambda_m^b \qquad (29)$$

Coefficient sandbox were determined in as a=0.9andb=7. The rated magnetizing current is 0.85 a (rms), and the rated magnetizing flux is 0.84524 Web (rms). The rated magnetizing inductance value is 0.9944 H. Using and the given data, the required Lmis easily obtained. The magnetizing curve of the machine and the magnetizing inductance variation are shown in Fig. 3.

4.SYSTEM IMPLEMENTATION

The basic configuration of the experimental system is shown in Fig. 4. It consists of an induction motor interfaced with a digital control board DS1102 based on a Texas InstrumentsTMS320C31 DSP for speed estimation. The induction motor is coupled with a dc generator for mechanical loading. The rating and parameters of the induction motor are given in the Appendix. Stator terminal voltages and currents are measured and filtered using analog circuitry. Hall-effect sensors are used for this purpose. The measured voltage and current signals are acquired by the A/D input ports of the DSP control board. This board is hosted by a personal computer on which mathematical algorithms are programmed and downloaded to the board for real-time speed estimation. A direct speed measurement is also carried out for comparison with the estimated speed. The output switching commands of the DSP control board are obtained actual speed feedback signal is replaced by

estimated one. The sensitivity to stator resistance mismatch

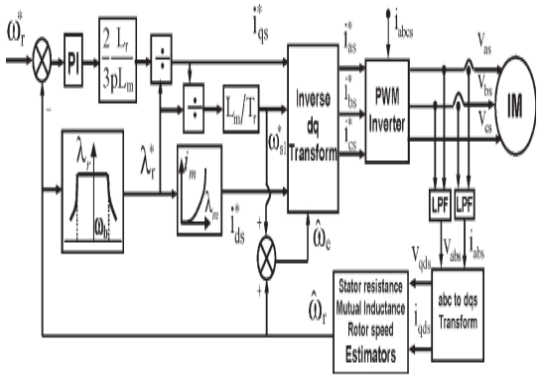

Fig. 5. IFO controller with compensation of flux saturation.

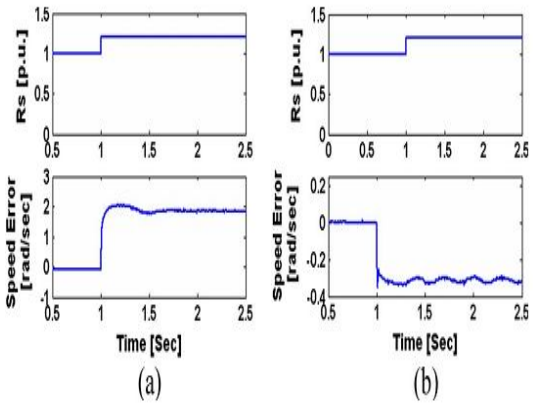

Fig. 6. Speed estimation error for +20% Rs error in the observer at (a) 150 rad/s and (b) 3 rad/s

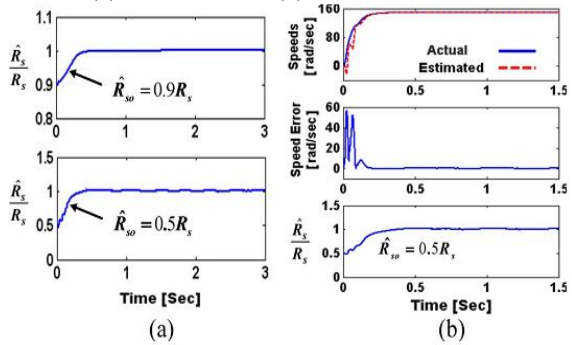

Fig. 7. (a) Stator resistance adaptation for−10% and−50%Rs initial detuning. (b) Actual and estimated speeds, and speed error for−50%R s initial detuning with stator resistance adaptation via its digital ports and interfaced with the inverter through op to isolated gate drive circuits.

5.RESULTS ANDDISCUSSION

A sensor less indirect field-oriented (IFO) controlled the is shown in Fig. 6 for+20%Rserror at high and low speeds. These results show that the speed estimation error at high-speed operation (150 rad/s) is 1.9 rad/s (1.26%), and that at low-speed operation (3 rad/s) is 0.32 rad/s (10.7%). Large error at low speeds may cause instability. In order to avoid this, the online stator resistance adaptation scheme (22) has been applied. The initial detuning in the stator resistance takes values of−10% and−50%, as shown in Fig. 7(a).

In both cases, the stator resistance adaptation was activated att=0. It is clear that the stator resistance estimator quickly removes the initial stator resistance error and consequently eliminates the large speed estimation error. A considerable reduction of the speed error is observed with stator resistance adaptation due to−50% initial Rs mismatch in the observer, as shown in Fig. 7(b).

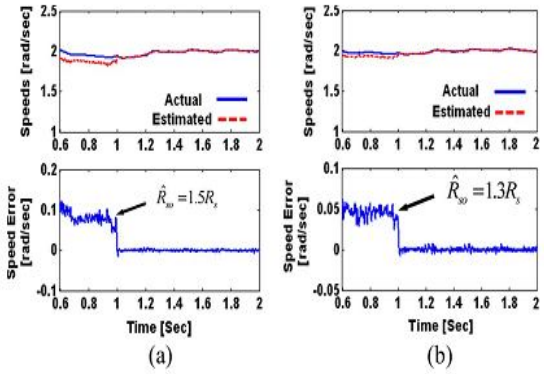

Fig. 8. Actual and estimated speeds, and speed estimation error at speedcommand of 2 rad/s. Stator resistance adaptation is activated at t=1s.(a) ˆ Rso=1.5Rs.(b)ˆ Rso=1.3Rs.

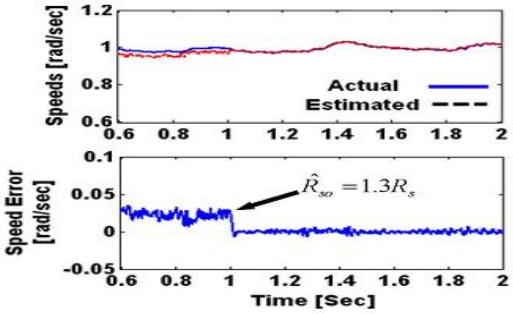

Fig. 9. Actual and estimated speeds, and speed estimation error at speed command of 1 rad/s. Stator resistance adaptation is activated at t=1s. ˆ Rso=1.3Rs.

Fig. 8 shows the actual and estimated speeds as well as the speed estimation error for two initial levels of stator resistance mismatch at a speed reference of 2 rad/s under no-load condition. The initial detuning in induction motor drive, shown in Fig. 5, is used, where the the stator resistance takes values of+50% and+30%. The same simulation results are obtained at a speed reference of 1 rad/s under no-load

condition, as shown in Fig. 9, with+30% initial detuning in the stator resistance. As shown, there exist substantial speed estimation error betweenthe actual and estimated speeds. The stator resistance adaptation scheme is turned on at t=1s. It is clear that activation of the stator resistance adaptation scheme quickly compensates for the initial error in the estimated stator resistance value and therefore eliminates the initial speed estimation error. The performance of identification schemes is also tested during speed reversal in the low-speed region. Fig. 10(a) shows the actual and estimated speeds as well as the speed estimation error during speed reversal from 0.5 to−0.5 rad/s. The correct value of stator resistance leads to elimination of the speed

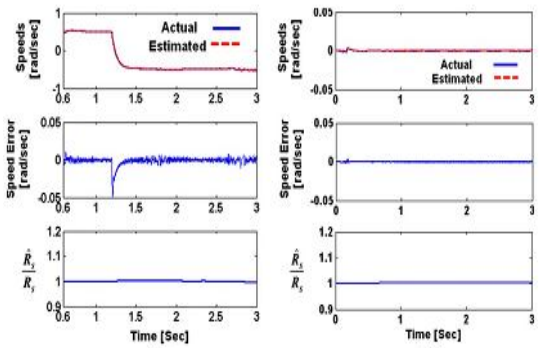

Fig. 10. Actual and estimated speeds, and speed estimation error with stator resistance tuning (a) during speed reversal from 0.5 to −0.5 rad/s and (b) at zero speed.

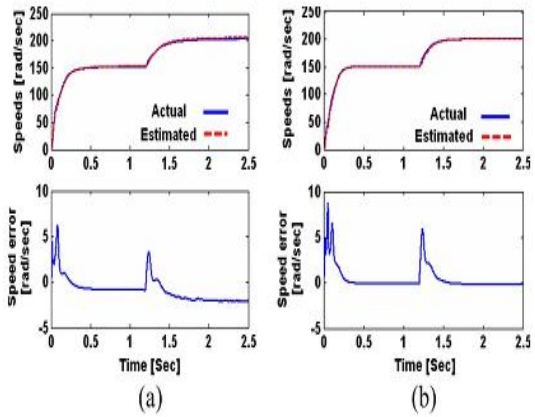

Fig. 11. Actual and estimated speeds, and speed estimation error for step change of speed command to 200 rad/s (a) with constant parameter SMO and (b) with modified SMO.

Estimation error and the actual and estimated speeds are in very good agreement in the steady state with a considerable reduction of the speed error (12.5%) during transients to zero in 0.25 s. Fig. 10(b) shows the actual and estimated speeds as well as the speed estimation error at zero speed with stator resistance tuning. As shown, the proposed speed observer with stator resistance adaptation achieves good speed estimation. Furthermore, results confirm that due to the accurate stator resistance estimation, the drive does not lose stability during operation at low and zero speeds. Finally, simulation results prove the supremacy of the parallel speed and stator resistance identification schemes to provide an accurate speed estimate in the very low speed region and also at zero speed. The IFO controller of Fig. 5 is also tested for the operation in the field-weakening region. Simulations are at first performed using the SMO of Fig. 2 with the magnetizing inductance set to the constant rated value which is suitable for the base-speed region. Speed reference is first applied to its rated speed value which equals 150 rad/s. Att=1.2s, the speed command is increased in step change to 200 rad/s, as shown in Fig. 11(a).This figure shows that the estimated speed tracks the actual speed in the base-speed region with minimum speed estimation error. However, once the field-weakening region is entered att=1.2s, a significant speed estimation error occurs due to variation of the magnetizing inductance that is neglected in the speed estimator. As shown, the speed estimation error changes

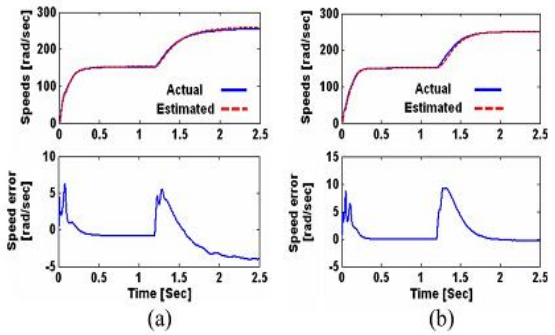

Fig. 12. Actual and estimated speeds, and speed estimation error for step change of speed command to 250 rad/s (a) with constant parameter SMO and (b) with modified SMO

From 0.6 to 2.25 rad/s at the final speed of 200 rad/s. The proposed modified SMO with online magnetizing inductance identification is now used instead of the constant parameter one. The observable differences of the actual and estimated speeds when compared with those of Fig. 11(a) are illustrated clearly from the speed estimation error shown in Fig. 11(b).It is observed from comparing the speed estimation error offing. 11(a) and (b) that the application of the modified SMO with online magnetizing inductance essentially eliminates the speed estimation error and gives accurate speed estimation in the field-weakening region. The same simulation results are repeated during step change from 150 to 250 rad/s in both cases, with constant magnetizing inductance [Fig. 12(a)] and with online magnetizing inductance identification instead of the constant parameter one [Fig. 12(b)]. Simulation results of Figs. 11

and 12 prove the ability of the modified SMO to adapt to the actual saturation level in the machine and therefore provide an accurate speed estimate for any operating point in the field-weakening region.

6.CONCLUSION

In this paper, parallel speed and stator resistance identification schemes of sensor less induction motor drives have been introduced to overcome the problem of resistance variation. Estimation algorithms have been obtained based on a sliding mode current observer combined with Popov's hyper stability theory. It has been found that activation of the stator resistance adaptation mechanism quickly compensates the initial error in the estimated stator resistance value and therefore eliminates the initial speed estimation error. As a consequence, the actual and estimated speeds become in very good agreement. Lowland zero-speed sensor less operations have also been investigated by the proposed SMO combined with the online stator resistance adaptation scheme. The supremacy of a certain speed estimation method is weighted by its successful operation and accuracy over a widespeed range. For this purpose, a modified SMO for speed estimation in the field-weakening region has been introduced.

The mismatch problem of magnetizing inductance due to rotor flux reference variation in the field-weakening region has been treated by an online identification algorithm. Using this algorithm, the magnetizing inductance has been continuously determined from the measured stator voltages and currents, enabling the correct calculation of rotor flux component at any operating point taking saturation level into consideration.

The superiority of the modified SMO over the constant parameter one for wide-speed-range estimation, from zero to high values beyond the base speed, has been proved by simulation results. This is also illustrated by the experimental results.

REFERENCES

APPENDIX

Magnetizing inductance. Ls; Lr Stator and rotor leakage inductances.RsStator resistance. Tr Rotor time constant .ωr; ˆ ωr Actual and estimated rotor speeds. σ Leakage coefficient. Actual and estimated stator current vectors.

INDUCTION MOTOR PARAMETERS

APPENDEX

LIST OF SYMBOLS	
L_m	Magnetizing inductance
$L_s; L_r$	Stator and rotor leakage inductances.
R_s	Stator resistance.
T_r	Rotor time constant
$\omega_r; \omega\hat{}_r$	Actual and estimated rotor speeds.
σ	Leakage coefficient
$i_s^s = [i_{ds}^s \quad i_{qs}^s]^T; i_s^s = [i\hat{}_{ds}^s \quad i\hat{}_{qs}^s]^T$	Actual and estimated stator current vectors.
$\lambda_r^s = [\lambda_{dr}^s \quad i_{qr}^s]^T; \lambda\hat{}_r^s = [\lambda\hat{}_{dr}^s \quad \lambda\hat{}_{qr}^s]^T$	Actual and estimated rotor flux vectors.
$v_s^s = [v_{ds}^s \quad v_{qs}^s]^T$	Stator voltage vector

$$A_{11} = aI \qquad A_{12} = cI + dJ \qquad A_{21} = eI$$

$$A_{22} = -\mathcal{E}A_{12} \qquad b_1 = bI$$

$$I = \begin{bmatrix} 1 & 0 \\ 0 & 1 \end{bmatrix} \qquad J = \begin{bmatrix} 0 & -1 \\ 1 & 0 \end{bmatrix}$$

$$a = -\left(\frac{R_s}{\sigma L_s} + \frac{L_m^2}{\sigma L_s T_r L_r}\right)$$

$$c = \frac{1}{\mathcal{E}T_r} \qquad d = \frac{\omega_r}{\mathcal{E}} \qquad e = \frac{L_m}{T_r}$$

$$\mathcal{E} = \frac{\sigma L_s L_r}{L_m} \qquad b = \frac{1}{\sigma L_s} \qquad \sigma = 1 - \frac{L_m^2}{L_s L_r} \qquad T_r = \frac{L_r}{R_r}.$$

Table 2
B. Induction Motor Parameters

Rated power(w)	250	$R_{s(p.u)}$	0.0658
Rated voltage(volt)	380	$R_{r(p.u)}$	0.0485
Rated current(Amp)	0.5	$L_{s(p.u)}$	0.6274
Rated frequency(Hz)	50	$L_{r(p.u)}$	0.6274
Number of poles	4	$L_{m(p.u)}$	0.5406

[1] J. Holtz, "Sensor less control of induction motor drives," Proc. IEEE, vol. 90, no. 8, pp. 1359–1394, Aug. 2002.

[2] M. S. Zany, M. M. Hater, H. Yasin, S. S. Shokralla, and A. El-Sabbe,"Speed-sensorless control of induction motor drives,"Eng. Res. J., vol. 30,no. 4, pp. 433–444, Oct. 2007.

[3] Q. Gao, G. Asher, and M. Sumner, "Senseless position and speed control of induction motors using high-frequency injection and without offline precommissioning, "IEEE Trans. Ind. Electron., vol. 54, no. 5, pp. 2474–2481, Oct. 2007.

[4] H. Tajima, G. Guide, and H. Umida, "Consideration about problems and solutions of speed estimation method and parameter tuning for speed sensor less vector control of induction motor drives," IEEE Trans. Ind. Appl., vol. 38, no. 5, pp. 1282–1289, Sep./Oct. 2002.

[5] J. Holtz and J. Quan, "Sensor less vector control of induction motors at very low speed using a nonlinear inverter model and parameter identification," IEEE Trans. Ind. Appl., vol. 38, no. 4, pp. 1087–1095,Jul./Aug. 2002.

[6] G. Guide and H. Umida, "A novel stator resistance estimation method for speed-sensor less induction motor drives,"IEEE Trans. Ind. Appl., vol. 36,no. 6, pp. 1619–1627, Nov./Dec. 2000.

[7] A. B. Proca, A. Keyhani, and J. M. Miller, "Sensor less sliding-mode control of induction motors using operating condition dependent models, "IEEE Trans. Energy Converts., vol. 18, no. 2, pp. 205–212, Jun. 2003.

[8] A. B. Proca and A. Keyhani, "Sliding-mode flux observer with online rotor parameter estimation for induction motors, "IEEE Trans. Ind. Electron., vol. 54, no. 2, pp. 716–723, Apr. 2007.

[9] D. P. Marketed and S. N. Vukosavic, "Speed-sensor less AC drives with the rotor time constant parameter update, "IEEE Trans. Ind. Electron., vol. 54,no. 5, pp. 2618–2625, May 2007.